International Journal of Humanoid Robotics
Vol. 4, No. 3 (2007) 549–573

World Scientific
www.worldscientific.com

"SOFT" EXOSKELETONS FOR UPPER AND LOWER BODY REHABILITATION — DESIGN, CONTROL AND TESTING

DARWIN G. CALDWELL* and N. G. TSAGARAKIS†

Italian Institute of Technology,
Genova, 16163, Italy
**darwin.caldwell@iit.it*
†*nikos.tsagarakis@iit.it*

SOPHIA KOUSIDOU‡, NELSON COSTA¶ and IOANNIS SARAKOGLOU‖

Centre of Robotics and Automation,
University of Salford,
Salford, M5 4WT, UK
‡*s.kousidou@pgr.salford.ac.uk*
¶*ncosta@solengin.com*
‖*i.sarakoglou@pgr.salford.ac.uk*

Received 9 March 2007
Revised 25 March 2007

The basic concepts for exoskeletal systems have been suggested for some time with applications ranging from construction, manufacturing and mining to rescue and emergency services. In recent years, research has been driven by possible uses in medical/rehabilitation and military applications. Yet there are still significant barriers to the effective use and exploitation of this technology. Among the most pertinent of these factors is the power and actuation system and its impact of control, strength, speed and, perhaps most critically, safety. This work describes the design, construction and testing of an ultra low-mass, full-body exoskeleton system having seven degrees of freedom (DOFs) for the upper limbs and five degrees of freedom (DOFs) for each of the lower limbs. This low mass is primarily due to the use of a new range of pneumatic muscle actuators as the power source for the system. The work presented will show how the system takes advantage of the inherent controllable compliance to produce a unit that is powerful, providing a wide range of functionality (motion and forces over an extended range) in a manner that has high safety integrity for the user. The general layout of both the upper and the lower body exoskeleton is presented together with results from preliminary experiments to demonstrate the potential of the device in limb retraining, rehabilitation and power assist (augmentation) operations.

Keywords: Exoskeleton; soft actuation; rehabilitation.

1. Introduction

Biological exoskeletons are common structures in both insects and crustaceans, where they form a hard outer casing that provides support or protection for the organisms allowing them to perform physical activities that, on a size-to-load

basis, could not be attempted by creatures with endoskeletons, e.g. humans. With robotic exoskeletons, the aim is to provide a structure that permits humans to make use of the concepts and advantages of an external skeleton and actuation to enhance power, endurance, or peak strength while retaining controlling human intelligence. These systems have the capacity to combine decision-making capabilities with machine dexterity and power, to greatly augment a person's physical abilities.

Yet, exoskeleton technology represents one of the most challenging areas of robotics research requiring significant advances in materials, mechanisms, electronics, sensors, controls, intelligence, communication, power sources and actuation — technology improvements that must be integrated together.[1,2] Further, the fundamental criteria for an exoskeleton, i.e. a mechanism that wraps around the operator's limbs allowing the replication or enhancement of forces at body segments, means that the human and the mechanical systems (robots) are inherently coupled and safety is paramount. It is therefore essential to provide drive systems that combine the positive attributes of conventional actuator design with a "softer" safer interaction capacity. These are features not found in traditional exoskeleton actuation (hydraulic or electric) but which are inherent in braided pneumatic muscle actuators (PMAs).[3] Using this format, exoskeletons can be developed for augmentation and rehabilitation applications (in particular) that have capabilities beyond those available with conventionally driven designs. This work will present the use of compliance regulated and controlled pairs of antagonistic PMAs to drive a combined whole-body exoskeleton incorporating both lower and upper body systems.

In this paper, we describe the construction and testing of a seven, degree of freedom (DOF) upper arm exoskeleton system and a ten-DOF lower body system. The total weight of the uncompensated upper arm system is less than 2 kg while the lower body system is less than 12 kg. This low mass is primarily due to the use of a new range of PMAs as the power source for the system. The need for safety, simplicity and lightness is met by this type of actuator, which also has an excellent power/weight ratio. The work presented will show how the system takes advantage of the inherent controllable compliance to produce a unit that is extremely powerful, providing a wide range of functionality (motion and forces over an extended range) in a manner that has high safety integrity for the user (patient). The general layout of the both upper and lower body exoskeleton is presented. This includes the design requirements, and the design description. The control issues of the system are also discussed. Initially, the low level joint control of the system is presented. A training control scheme is introduced which is used to control the exoskeleton. Results from preliminary experiments demonstrate the potential of the device in limb retraining, rehabilitation and power assist (exoskeleton) operations.

2. Historical Development

Some of the first exoskeletons (both fictional and real) were suggested and built in the 1960s and often had a military dominated theme. The hydraulically powered

Green-man exoskeleton was designed for the US Army for performance augmentation. Designed as a forklift truck replacement, but with greater flexibility, mobility and dexterity, it was beset by many problems with the mass of the power pack and the hydraulics and was never deployed. In 1965, General Electric developed Hardiman, a 700 kg, 30-jointed system powered by both hydraulics and electric motors. Again, this system was too large and heavy with severe stability problems.[2]

These early efforts suffered from fundamental technological difficulties, such as: computation speeds which were insufficient to provide the control functions necessary to give smooth and effective tracking of the wearer's input movements; energy supplies that were not compact and light enough to be easily portable; actuators that were too sluggish, heavy, and bulky.[4]

There was a significant loss of momentum after these set-backs and research in large-scale exoskeletons was largely forgotten, apart from the work of Kazerooni in force extenders, until the late 1980s and early 1990s when developments in virtual reality and telepresence prompted renewed developments looking at both portable and fixed base exoskeletons. Military requirements were again to the fore but in this instance the focus was on upper limb systems as opposed to legged or whole-body units.[5,6] The EXOS ArmMaster had five active DC powered DOFs and additional passive DOFs to increase comfort and permit size adjustment.[2] Output torques ranged from 0.38 Nm to 6.3 Nm with a total mass of approximately 10 kg.

The Force REFLecting EXoskeleton (FREFLEX) is a seven-DOF DC motor powered exoskeleton with a workspace of approximately 125 cm × 100 cm × 75 cm and an output force of at least 25 N. The FREEFLEX is a non-portable system.[7] The hydraulically powered, seven-DOF Sarcos Arm Master developed for subsea teleoperation is one of the most powerful of all the exoskeletons. In addition to the seven-DOF in the arm, there are three additional DOFs to allow control of the thumb and one finger. The actuators provide output torques that range from 97.7 Nm for the shoulder, to 5.5 Nm for the hand joints. Due to the power of this system, safety mechanisms were incorporated, including mechanical joint limits, dead man switches and "watch dog" routines.[8] The four-DOF SMU exoskeleton has three DOFs at the shoulder and one DOF at the elbow. Force feedback is generated by means of pneumatic cylinders. To support its weight, active gravity compensation is used, which is controlled from a neural network based controller.[2,7]

Within Europe, the GLAD-IN-ART exoskeleton is a seven-DOF DC motor powered exoskeleton having a configuration broadly similar to the EXOS with one extra DOF for forearm pronation/supination and two DOFs at the wrist. The torque output ranges from 20 Nm for the shoulder to 10 Nm for the upper arm rotation and elbow flexion extension joint and 2 Nm for the forearm joints. The unit again weighs 10 kg but has active gravity compensation to offset this loading.[9] Other notable systems include the KIST exoskeleton with nine DOFs (seven rotational and two prismatic joints) powered by pneumatic cylinders[10] and the seven-DOF DC motor powered Sensor Arm II exoskeleton developed at the University of Tokyo.[11]

In recent years, there has once again been renewed military interest in exoskeletons with DARPA funding a wearable robotic system to help soldiers carry heavier loads. Two programs in particular have addressed this problem. Bleex 1 and 2 have two electromechanical legs that strap to the outside of the wearer's legs. These systems have good user maneuverability, permitting users to walk, squat, twist, kneel and run at speeds exceeding 2 m/s while carrying a payload of 45 kg. Bleex 2 is a compact and lightweight (14 kg) hydraulically powered design.[12] The Sarcos robotic system is reported to be able to carry 84 kg with no user perception of load. The system permits walking and running and can react to disturbance inputs, e.g. stumbling. The exoskeleton uses a special internal-combustion engine that can use a variety of fuels and deliver enough hydraulic power to meet the strength and speed requirements of the robotic limbs.[13]

In non-military applications, one of the most important systems is the HAL (short for Hybrid Assistive Limb) full-body suit designed to aid people who have degenerated muscles or those paralyzed by brain or spinal injuries. HAL-5 is constructed from a nickel molybdenum and extra-super-duralumin frame, strengthened by plastic casing. The metal frame is strapped to the body and supports the wearer externally, its several electric motors acting as the suit's muscles to provide powered assistance to the wearer's limbs. The exoskeleton is powered by both nickel-metal hydride and lithium battery packs giving almost three hours continuous operation. HAL-5 weighs about 21 kg.[13]

From a medical rehabilitation perspective there have been a number of developments both for lower and upper body. Much of the early pioneering work was developed by Vukobratovic.[4] About the same time, the Balanced Forearm Orthosis (BFO) was developed as a wheelchair mounted passive device to enable a person with weak musculature to move their arms in the horizontal planes.[14] In 1975, the Burke rehabilitation centre developed a five-DOF version of the BFO powered by means of electric motors, but this never gained significant acceptance.[15] The Hybrid Arm Orthosis (HAO), developed by the authors of Ref. 16, aimed to provide upper arm motion assistance. This system offered shoulder abduction and elbow flexion, wrist supination and a three joint jaw chunk pinch. The shoulder and the elbow joints were body powered while the wrist supination and the three-point jaw chuck pinch power were generated by two separate DC motors. More recently, a system developed at MEL[17] used a parallel mechanism to suspend the upper arm at the elbow and wrist level. Each point was suspended by an overhanging plate using three strings arranged in parallel.

Among the most interesting of the powered orthosis systems is a motorized upper limb orthosis system (MULOS) developed at the University of Newcastle in mid-1990s.[18,19] The system has five DOFs and is designed to work in three different modalities: Assistive, Continues Passive Motion (CPM) and Exercise. This device appeared to have good potential but development was discontinued in 1997.

MIT MANUS is another robotic system that was developed for the physical therapy of stroke victims. The system supports up to five DOFs through two separate

modules. Although it is claimed to be portable, its weight is around 45 kg.[20–21] The system developed by the authors of Ref. 22 was also designed to provide upper limb motion assistance. This system provides eight DOFs supporting upper limb and hand. Special care was taken in the design of the system to ensure user safety.

The ARM Guide[23,24] consists of an instrumented linear constraint that can be oriented in different directions across the subject's workspace using a three-spline steel shaft. This device was primary used as a measurement tool for force and motion during mechanically guided movement. The most recent system of all is the GENTLE project, which uses a haptic master device to provide exercise for an arm using an interactive virtual environment. The system has six DOFs, but only the three translational motions are active.[25]

3. Design Requirements

Based on the knowledge of the state of the art as well as user needs for safe, compliant powered actuation for both rehabilitation and human performance augmentation applications, fundamental technical specifications could be developed.[26] These requirements focused on:

(i) *A structure having low mass/inertia.* The mass of the exoskeleton must be minimized, to enhance user comfort, portability and to reduce energy wastage in simply moving the structure. Low mass and inertia also have secondary benefits when considering the safety aspects of what is in essence a robot physically attached to the human.

(ii) *Safety.* As the system is in direct contact with the human operator the safety requirement is paramount. Safety is enhanced through low mass/inertia structures that combine high strength with actuator and/or structural compliance. The device must be safe technically and perceived as safe by potential users.

(iii) *Comfort of wearing.* As the extended use of the device is certainly possible and probably necessary, the device must be comfortable, causing no fatigue to the operator even after long periods, e.g. 1–2 hours of operation. This requirement should include ease of fitting adjustment and removal.

(iv) *Extensive range of motion.* A generic specification for the display range of motion can be defined as the "typical" human workspace.

(v) *Accurate force feedback.* Accurate representation of the forces means that the device must have sufficient force resolution capabilities. The human arm force resolution capability for the different arm joints has been studied. Experiments from Ref. 27 revealed that the average force resolution is around 0.36 N and tended to increase as the target force increases. Using this as a specification value will ensure that the operator feels no force discontinuities during motion.

(vi) *Good motion sensing resolution.* The motion sensing requirements of the device obviously depend on the position resolution capabilities of the human. Since the

human position sensing resolution varies for different joints in the human body, the motion sensing resolution will be determined by the sensing capabilities of the part of the body that the system is attached to. These values are typically in the range 0.8°–2.0°.[27,28]

(vii) *Accurate automatic compensation for gravity forces.* Since medical applications will involve individuals with at best weakened arm structures, active, easily updated gravity compensation forms a keystone of the design.

(viii) *Reliability.* As with all systems, user acceptance is dependent to a large extent on the reliability and utility of the mechanism. It is therefore vital that appropriate design concerns are given to reliability in all operations and in environments where materials like water, dust or grease are presented.

(ix) *Complexity.* As with most designs, options that keep complexity to a minimum will tend to improve reliability, and reduce cost and these should always be under consideration during the design process.

4. Mechanical Design

The mechanical structure is formed in two major portions, an upper body exoskeleton to provide power to the arm and a lower body exoskeleton to provide augmentation to the legs during walking activities. In both instances, the primary design goal has been for aspects of rehabilitation. For the upper body, the scenario is rehabilitation after strokes while for the lower body paralysis, muscle wastage and stroke are the main targets. At the same time, the structure is capable of performing the general aspects of human performance augmentation. A hand exoskeleton has also been developed and is shown in later figures but is not described in this paper.[29]

4.1. *Upper body*

The mechanical arm structure has seven DOFs corresponding to the natural motion of the human arm from the shoulder to the wrist but excluding the hand. The structure which is constructed primarily from aluminium and composite materials, with high stress joint sections fabricated in steel has three DOFs in the shoulder (flexion/extension, abduction-adduction and lateral-medial rotation), two DOFs at the elbow permitting flexion/extension, pronation/supination of the forearm, and two DOFs at the wrist (flexion-extension and abduction-adduction); Fig. 1.

The arm is constructed for use by a "typical adult" with only minor changes to the set-up. Arm link length changes can easily and quickly be effected, if necessary making it easy to accommodate a range of users, which is an important aspect of the design. The arm is attached to the user arm at the elbow and wrist level using two wide velcro bands. This was found to be adequate during operation, providing a secure attachment together with easiness of system donning and removal.[30] High

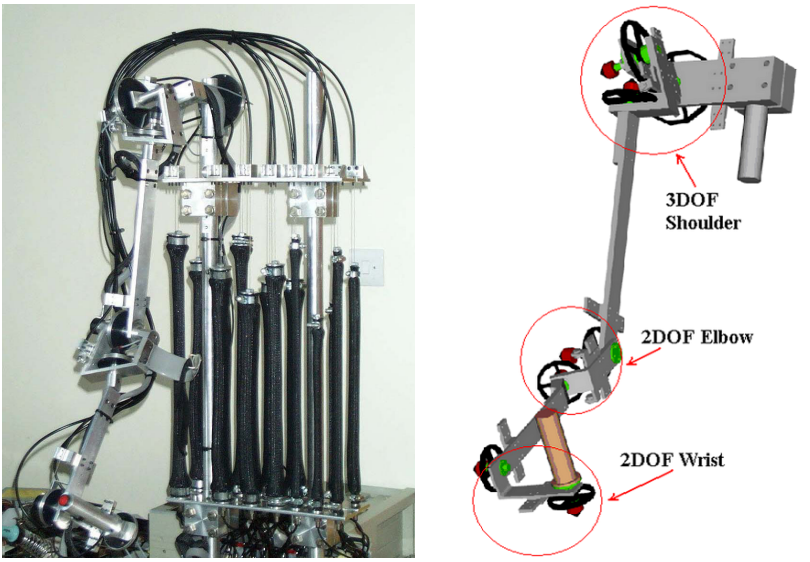

(a) Arm exoskeleton structure. (b) Exoskeleton mechanical chain.

Fig. 1. Upper limb mechanical structures.

linearity sensors provide position sensing on each joint, with joint torque sensing achieved by integrating two strain gauges (mounted on internal spokes) inside each joint pulley. Ranges of motions of the arm exoskeleton and forces generated are shown in Table 1.[31]

4.2. *Lower body*

The design concepts and principles of the upper body that have been adopted were reasonable in the lower body design. The mechanical structure, which is once again constructed primarily from aluminium with joint sections fabricated in steel, consists of a ten-DOF (five DOFs per leg) mechanism corresponding to the fundamental natural motion and range of the human legs from the hip to the ankle, but excluding lower leg rotation and ankle flexion/extension.

The hip structure has three DOFs as in the shoulder (flexion/extension, abduction-adduction and lateral-medial rotation), one DOF at the knee permitting flexion/extension, and one DOF at ankle (dorsi/plantar flexion); Fig. 2. The leg is mounted in a moulded lower body brace which is light, low cost and comfortable, designed for ease of change of leg link length. The overall mass of the system is less than 12 kg.[32] As with electrical systems, it must be recognized that this mass does not include the power source. Ranges of motions of the lower body exoskeleton and forces generated are shown in Table 1. The total weight of the exoskeleton consisting of the both legs and a rigid spine is 12 kg assembled with a length of

Table 1. Motion ranges for the training/rehabilitation arm.

Motion	Human Arm (°)	Exo + Human Arm (°)	Human Isometric Strength	Achieved Torque Peak (Min)	Leg Motion	Range (°)	Force
Wrist flexion	90	70	19.8 Nm	28 Nm (5 Nm)	Plantar Flexion	50	60 Nm
Wrist extension	99	70			Dorsi flexion	30	
Wrist adduction	27	30	20.8 Nm	24 Nm			
Wrist abduction	47	45		(7 Nm)			
Forearm supination	113	45	9.1 Nm	25 Nm			
Forearm pronation	77	40		(9 Nm)			
Elbow flexion	142	100	72.5 Nm	76 Nm (19 Nm)	Knee	140	60 Nm
Shoulder flexion	188	110	110 Nm	95 Nm	Hip flexion	120	60 Nm
Shoulder extension	61	25		(30 Nm)	Hip extension	20	
Shoulder adduction	48	20	125 Nm	128 Nm	Hip adduction	30	65 Nm
Shoulder abduction	134	100		(27 Nm)	Hip abduction	45	
Shoulder medial rotation	97	48		46 Nm (5 Nm)	Hip int. rot.	45	
Shoulder lateral rotation	34	46			Hip ext. rot.	50	

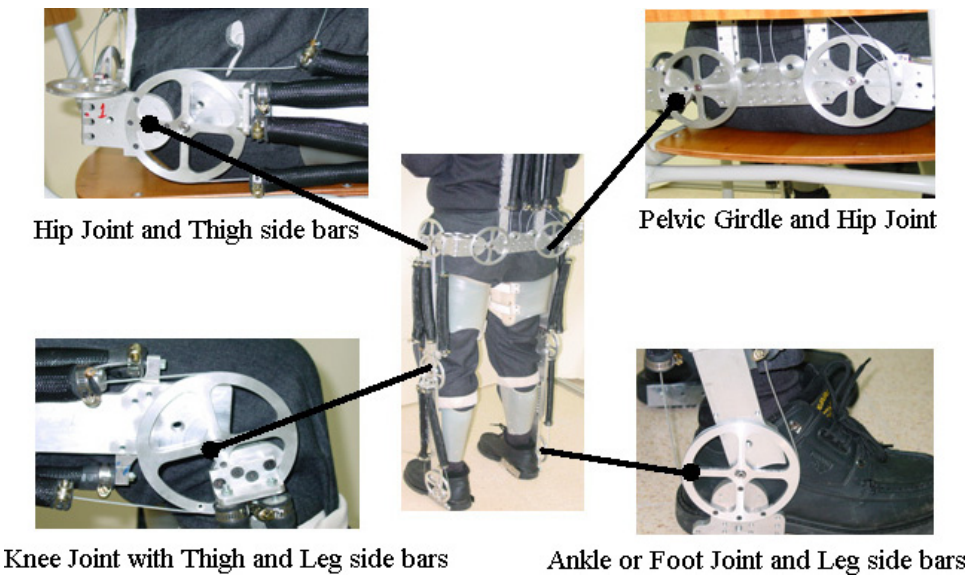

Fig. 2. Lower limb exoskeleton mechanical structure.

520 mm from the hip to the knee while the length from the ankle's base to the top of the knee is 500 mm.

4.3. *Actuator design*

As identified in the failings of the early Hardiman and Greenman systems, actuators and actuation systems are essential, perhaps defining, parts of all exoskeleton structures, providing the forces, torques and mechanical motions needed to move the joints, limbs or body. Their performance is usually characterized by parameters such as power (particularly power/weight and power/volume ratios), strength, response rate, physical size, speed of motion, reliability, controllability, compliance and cost. The nature of the drive source proposed in this work forms a key sub-system making use of "soft" compliant actuator technology that permits a change in the operational paradigm for the design and use of the exoskeletons. This is fundamentally different from methods previously developed and is a key to the success of this technique. This system uses braided pneumatic muscle actuators (PMAs) that provide a clean, low cost actuation source with a high power-to-weight ratio and safety due to the inherent compliance. These PMAs are constructed as a two-layered cylinder; Fig. 3.

This design has an inner rubber liner, an outer containment layer of braided nylon and endcaps that seal the open ends of the muscle. Within the actuator, pressure sensors, have been incorporated to monitor the internal state of the muscle, while miniature strain gauge based load cells can be used to directly measure the force in any actuation system. The complete unit can safely withstand pressures up to 700 kPa (7 bar), although 600 kPa (6 bar) is the operating pressure for this system. The detailed construction, operation, and mathematical analysis of these actuators can be found in Refs. 33 and 34. The structure of the muscles gives the actuator a number of desirable characteristics:

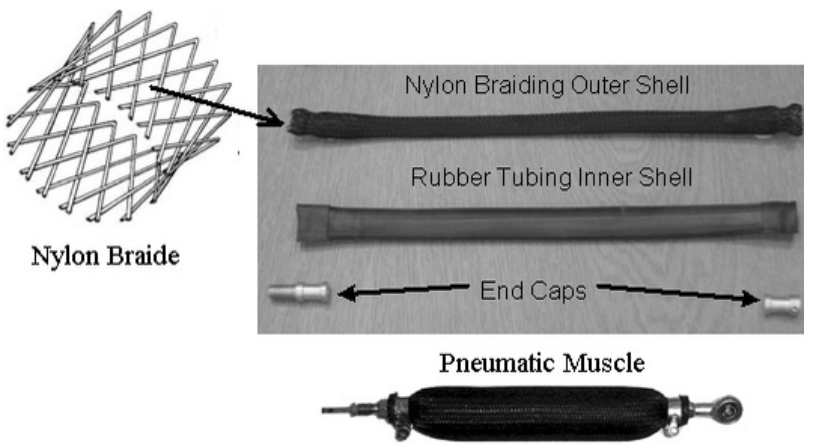

Fig. 3. Pneumatic muscle actuator design.

(i) Muscles can be produced in a range of lengths and diameters with larger sizes producing larger contractile force.
(ii) The actuators have exceptionally high power and force to weight/volume ratios $> 1\,\mathrm{kW/kg}$.
(iii) The actual achievable displacement (contraction) is dependent on the construction and loading but is typical 30%–35% of the dilated length — comparable with the contraction achievable with natural muscle.
(iv) "Soft" construction and finite maximum contraction make PMAs safe for human–machine interaction.
(v) Controllers developed for the muscle systems have shown them to be controllable to an accuracy of better than 1% of displacement.
(vi) Bandwidth for antagonistic pairs of muscles of up to 5 Hz can be achieved.
(vii) Force control using antagonistic pairs for compliance regulation is possible as for natural muscle.
(viii) When compared directly with human muscle, the contractile force for a given cross-sectional area of actuator can be over $300\,\mathrm{N/cm^2}$ for the PMA compared to 20–$40\,\mathrm{N/cm^2}$ for natural muscle.
(ix) The actuators can operate safely in aquatic, dusty or other liquid environments.
(x) The actuators are highly tolerant of mechanical (rotational and translational) misalignment, reducing the engineering complexity and cost.

It is worth noting that a commercial form of the PMA with characteristics similar to the PMA is available from Festo. While it is possible to use these actuators, they were not selected since in-house manufacture permits greater control over the dimensions, forces and general performance of the drives, allowing them to be tailored to this application.

4.4. *Actuator attachments*

Joint motion/torque is achieved by producing appropriate antagonistic torques through cables and pulleys driven by the pneumatic actuators. Since the PMA is a single direction-acting element (contraction only), this means that for bidirectional motion/force two elements are needed. These two acting elements work together in an antagonistic scheme simulating a biceps-triceps system to provide the bidirectional motion/force; Fig. 4.

In the above set-up, $L_{\min}$ denotes the length of the muscle when it is fully contracted; $L_0 = L_{\min} + \frac{L_{\max} - L_{\min}}{2}$ is the initial dilated length of muscle, which is equal to half of maximum muscle displacement needed to maximize the range of motion of the joint; $L_{\max}$ is the maximum dilated length; r is the radius of the pulley; and P_1, P_2 are the gauge pressures inside the two muscles.

Flexible steel cables are used for the coupling between the muscles and the pulley. Since most of the joints require a range of rotation in excess of 90°, double groove pulleys have been employed. The pulleys have been made from solid aluminium

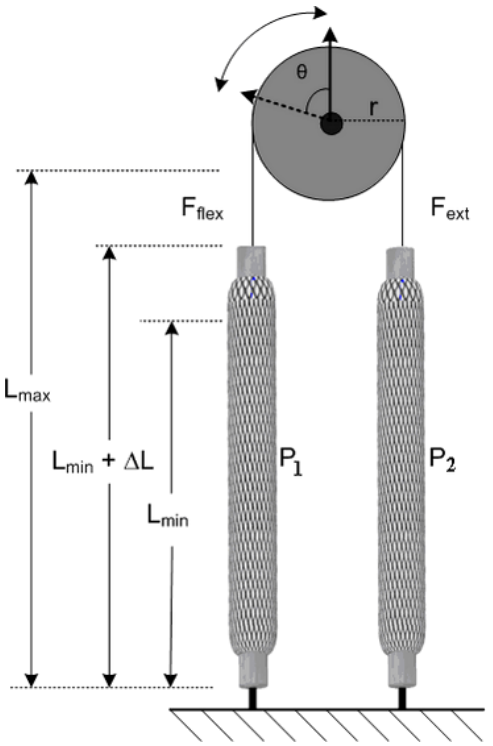

Fig. 4. Antagonistic pairs of muscles.

pieces internally machined to form a four spoke structure. On each of these internal spokes, strain gauges are mounted to form a joint torque sensor. The compact actuator structure allows for integration close to their respective powered joints. This makes the overall design compact, in line with the design requirements. The muscles used in the upper limb have a diameter of 2–4 cm with an "at rest" length of 15–45 cm.

For the lower limb systems, the ankle actuators (two actuators) and the lower leg flexion/extension actuator (two actuators) are mounted on the side. The knee actuators (two actuators) and the leg hip rotation actuators (two actuators) are mounted on the thigh side while the hip actuators (four actuators) are mounted on the body brace behind the operator's back. The muscles used in this project have a diameter of 2 cm, with an "at rest" length of 50–70 cm.

4.5. *System controller and user interface*

The activation of the PMA is reliant on the effective control of the airflow into and from the muscles. This is controlled by MATRIX valves that incorporate four 3/3 controllable ports in a package having dimensions of 45 mm × 55 mm × 55 mm and weighing less than 320 g. The valves can be driven and controlled at up to

400 Hz PWM signal providing rapid, smooth motion. Development of an adaptive controller and details of the design can be found in Ref. 33. By incorporating a pressure sensor into the valve inlet, closed loop pressure control is also possible. Pulsing of the valves along with data collection from the position, pressure and torque sensors is controlled from local dedicated microcontrollers with I/O, ADC and communication port facilities. The external PC is used to supervise the working conditions of the prototype.

Specifically, each individual muscle pairs (joint) are controlled by a local DSP which is again designed to mate with the valve assembly for compact operation. Each MCU controls up to eight PMAs (eight inlets + eight outlets). The DSPs are connected through a data bus to the interface PC, running Windows based monitoring software.

5. Modeling and Control

5.1. *Modeling of the pneumatic muscle actuated joint*

To make effective use of the "soft" properties of the PMAs, accurate modeling and control is essential and extensive work has sought to achieve this. Two main approaches to the force generation problem for the PMAs have been developed by researchers, with the first based on energy modeling,[35] and the second using force profiles of the surface pressure.[33,34] Both methods provide the same base model described by the following equation:

$$F = \frac{\pi D_0^2 P}{4}(3\cos^2(\theta) - 1), \tag{1}$$

where θ is the braid interweave angle, D_0 is the maximum theoretical muscle diameter at a braid interweave angle of $\theta = 90^o$ and P is the operating pressure. Modeling of the joint dynamics based on a simplified muscle model derived from Eq. (1) considers the PMAs as a nonlinear spring with an elastic constant that is related to the muscle properties. Equation (1) can be written as a function of the muscle length L and the length of one thread of the braided structure b as

$$F = \frac{\pi D_0^2 P(3L^2 - b^2)}{4b^2}. \tag{2}$$

Simulated results using the above equation and experimental data (Fig. 5) for different sizes of muscles suggest that the pneumatic muscle behaves like a pressure dependent variable compliance spring. Based on this observation and considering constant pressure due to the small length change dL, the muscle spring stiffness per unit length can be computed from Eq. (2):

$$K = \frac{dF}{dL} = \frac{6\pi D_0^2 PL}{4b^2}. \tag{3}$$

As can be seen from Eq. (3) the stiffness of the muscle is a function of the operating pressure P and the length of the muscle L. We can now calculate the stiffness per

unit pressure K_{pr}:

$$K_{\mathrm{pr}} = \frac{dK}{dP} = \frac{6\pi D_0^2 L}{4b^2} = K_{\mathrm{gas}} L. \tag{4}$$

The muscle force equation can now be rewritten to replicate a spring force equation:

$$F = K_{\mathrm{pr}} P\,(L - L_{\min}), \tag{5}$$

where $L_{\min}$ is the length of the muscle when it is fully contracted. Equation (5) represents the muscle as a nonlinear quadratic spring. The muscle force equation in the form presented above is used for the modeling of the pneumatic muscle actuated joints of the compliant arm haptic system. Based on the static force equation of the PMA, the state space model of the joint powered by two antagonistic muscles can be computed. The equation that describes the motion of the joint is given by

$$J\ddot{\theta} + D\dot{\theta} = \tau, \tag{6}$$

where J, D and τ denote the joint inertia, damping and torque, respectively. Considering now the antagonistic pair of muscles shown in Fig. 5 and using the muscle force equation (5), the forces developed are given by

$$\begin{aligned} F_1 &= K_{\mathrm{pr}} P_1 (L_0 - L_{\min} + r\theta), \\ F_2 &= K_{\mathrm{pr}} P_2 (L_0 - L_{\min} - r\theta). \end{aligned} \tag{7}$$

Equations (7) can be rewritten as

$$\begin{aligned} F_1 &= K_{\mathrm{pr}} P_1 (\Delta L_0 + r\theta) = K_{\mathrm{gas}} P_1 L_1 \Delta L_1, \\ F_2 &= K_{\mathrm{pr}} P_2 (\Delta L_0 - r\theta) = K_{\mathrm{gas}} P_2 L_2 \Delta L_2, \end{aligned} \tag{8}$$

where $\Delta L_0 = L_0 - L_{\min} = \frac{L_{\max} - L_{\min}}{2}$ is the initial dilation for the muscles and $L_1 = L_{\min} + \Delta L_1$, $L_2 = L_{\min} + \Delta L_2$ are the lengths of the muscles at any joint positions.

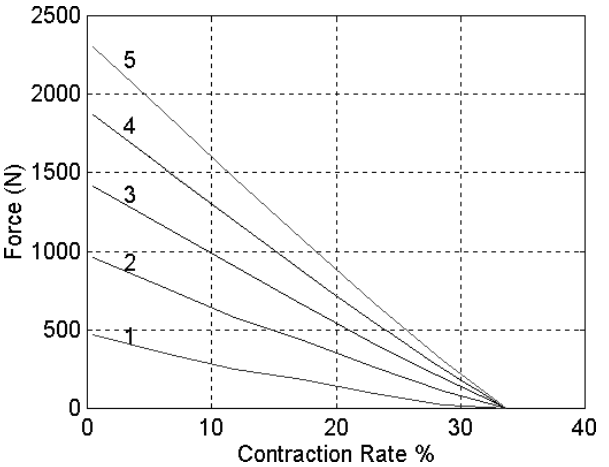

Fig. 5. Experimental force/displacement profiles.

The dilations for the two muscles at any joint position are $\Delta L_1 = \Delta L_0 + r\theta$ and $\Delta L_1 = \Delta L_0 - r\theta$. Using (8), the torque developed at the joint can now be computed:

$$T = (F_2 - F_1)\, r = (K_{\text{gas}} P_2 L_2 \Delta L_2 - K_{\text{gas}} P_1 L_1 \Delta L_1)\, r. \tag{9}$$

The equation of motion of the single joint in Fig. 5 can be written as

$$\ddot{\theta} = \frac{-D}{J}\dot{\theta} + \frac{K_{\text{gas}} r^3 (P_2 - P_1)}{J}\theta^2 - \frac{K_{\text{gas}} r^2 (P_2 + P_1)(2\Delta L_0 + L_{\min})}{J}\theta + \frac{K_{\text{gas}} r (P_2 - P_1)\Delta L_0 (L_{\min} + \Delta L_0)}{J}. \tag{10}$$

By selecting the states of the system to be $x_1 = \theta$ and $x_2 = \dot{\theta}$, the state equations of the system can be formulated from (10) as

$$\begin{bmatrix} \dot{x}_1 \\ \dot{x}_2 \end{bmatrix} = \begin{bmatrix} 0 & 1 \\ \dfrac{K_{\text{gas}} r^3 (P_2 - P_1)}{J} x_1 - \dfrac{K_{\text{gas}} r^2 (P_1 + P_2) L_{\max}}{J} & -\dfrac{D}{J} \end{bmatrix} \begin{bmatrix} x_1 \\ x_2 \end{bmatrix} + \begin{bmatrix} 0 \\ \dfrac{K_{\text{gas}} r (L_{\max}^2 - L_{\min}^2)}{4J} \end{bmatrix} [P_2 - P_1]. \tag{11}$$

The above joint model describes the joint dynamics but since it is based on the static force equation of a PMA it does not incorporate the dynamics of the actuator air pressures P_1 and P_2. In this system, the air pressure inside each of the two muscles is regulated using on/off solenoid 3/3 valves; Fig. 6.

As can be seen from Fig. 8, a PID controller is used to calculate the on/off times of the venting/filling valves and effectively regulates the pressure. The dynamics of each of the two pressure regulators for P_1 and P_2 can be identified in MATLAB using experimental input/output pressure data from each muscle and can be finally incorporated into the control scheme.

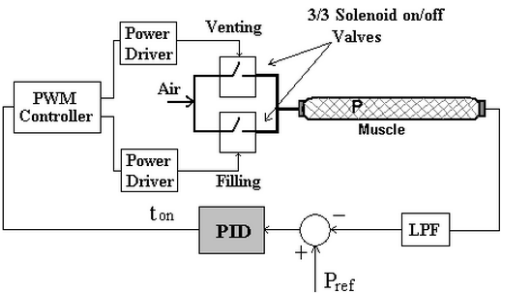

Fig. 6. Control scheme of the muscle pressure using on/off solenoid valves.

5.2. *Joint model verification*

To verify the joint model developed in the previous section, the open loop step response of one of the system's joints was recorded and the outcome of the model (11) was compared with the experimental data. The air pressure was controlled using pulse width modulation with a switching frequency up to 200 Hz and a fast response time of less than 2 ms. The open loop step response of the system to the input pressure variation $\Delta P = P_{\text{ref}_2} - P_{\text{ref}_1}$ was recorded. The two pressure references $(P_{\text{ref}_1}, P_{\text{ref}_2})$ were set as

$$(P_{\text{ref}_1}, P_{\text{ref}_2}) = \left(\frac{P_{\max} - \Delta P}{2}, \frac{P_{\max} + \Delta P}{2} \right), \tag{12}$$

with $P_{\max} = 400{,}000$ (Pa). This gives a balanced input pressure variation and the system can be considered as a SISO system. The same generated $\Delta P \in [-100000\ 100000]$ (Pa) profile was used as input for the theoretical system model, and the theoretical step response generated by MATLAB was plotted against the experimental one in Fig. 7.

Figure 8 shows a good transient equivalence between the theoretical and the experimental responses. A steady state error between the two responses can be observed which is believed to be due to the non-modeled system parameters (e.g. pressure dynamics, delays, friction, saturation, etc.).

5.3. *Upper limb exoskeleton impedance control scheme*

When operating in an assistive/augmentation (or resistive for exercise) mode, an impedance control scheme is employed for the overall exoskeleton system to enable execution of complex assistive/resistive exercises. The following equation describes

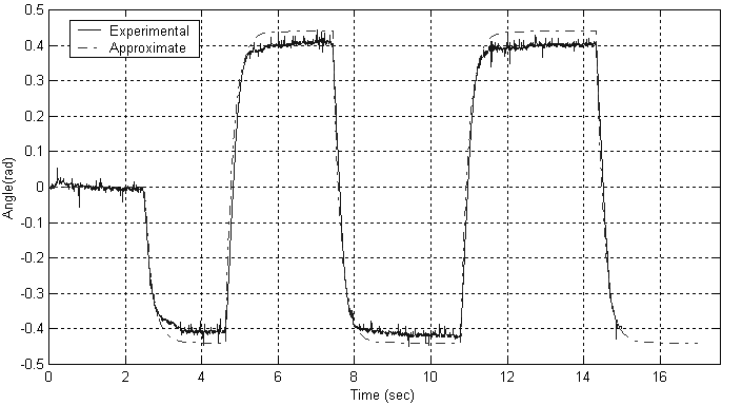

Fig. 7. Experimental and theoretical step response.

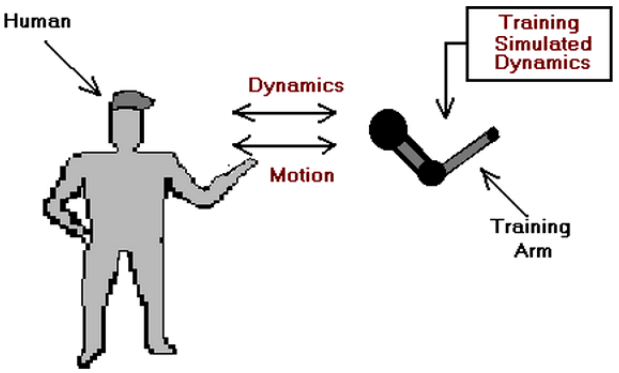

Fig. 8. Schematic diagram of the human and exoskeleton.

the dynamic behavior of the exoskeleton:

$$M(q) \cdot \ddot{q} + V(q, \dot{q}) + F(\dot{q}) + G(q) + J^T \cdot F_R = \tau_{\text{joint}}, \tag{13}$$

where q is the joint variable n-vector, τ_{joint} is the joint torque vector, $M(q)$ is the inertia matrix, $V(q, \dot{q})$ is the coriolis/centripetal vector, $F(\dot{q})$ is the friction vector, $G(q)$ is the gravity vector, F_R is the force that the arm generates at the end-tip, and J^T is the transpose Jacobian of the exoskeleton.

The above equation can be used to describe the interaction between an operator and the exoskeleton. Considering the scenario described in Fig. 8, where the user's limb is attached to the exoskeleton.

Let F_H denote the force that the human exerts on the exoskeleton arm endtip (which is actually the force felt by the user), F_R is the force that the exoskeleton applies to the operator, and $Z_E(s)$ is the system's simulated mechanical impedance. To make the operator feel the simulated augmentation/resistive dynamics, the following equation must be applied:

$$Z_E(s) \cdot (x - x_E) = M_E \cdot \ddot{x} + B_E \cdot \dot{x} + K_E \cdot (x - x_E) = F_H, \tag{14}$$

where M_E, B_E, and K_E are the inertia, damping, and stiffness coefficients. The above equation defines the desired characteristics of the motion of the pair (**Operator, Exoskeleton**). Having specified the desired behavior of the system, the control law can now be derived by eliminating $\ddot{x}$ and $\ddot{q}$ from Eqs. (13) and (14). To do this, the following equations, which relate the velocities and accelerations of the exoskeletal trainer end-point with the velocities and accelerations in joint space, are introduced:

$$x = J \cdot \dot{q}, \tag{15}$$

$$\ddot{x} = J \cdot \ddot{q} + \dot{J} \cdot \dot{q}. \tag{16}$$

Solving Eqs. (14) and (16) for $\ddot{x}$ and $\ddot{q}$, respectively, gives

$$\ddot{x} = M_E^{-1} \cdot (F_H - B_E \cdot \dot{x} - K_E \cdot (x - x_E)), \tag{17}$$

$$\ddot{q} = J^{-1} \cdot (\ddot{x} - \dot{J} \cdot \dot{q}). \tag{18}$$

Combining Eqs. (13), (17) and (18), $\ddot{q}$ can be eliminated to give

$$M(q) \cdot J^{-1} \cdot (M_E^{-1} \cdot (F_H - B_E \cdot \dot{x} - K_E \cdot (x - x_E)) - \dot{J} \cdot \dot{q}) + G(q) = \tau_{\text{joint}} - J^T \cdot F_R. \tag{19}$$

To keep the cartesian inertia of the human arm/exoskeleton unchanged:

$$M_E = J^{-1} \cdot M \cdot J^{-T}. \tag{20}$$

Considering slow motions typical in rehabilitation applications and that $F_R = -F_H$, Eq. (19) gives

$$\tau_{\text{joint}} = -J^T \cdot (B_E \cdot \dot{x} + K_E \cdot (x - x_E)) + G(q). \tag{21}$$

The above equation describes the impedance control law for the overall upper limb exoskeleton. The damping and the stiffness matrixes B_E and K_E are 6×6 diagonal matrices and depend on the dynamics to be modeled. To enable effects such as static force to be simulated, the control equation (21) can be modified by including a bias force matrix F_{bias} as follows:

$$\tau_{\text{joint}} = -J^T \cdot (B_E \cdot \dot{x} + K_E \cdot (x - x_E) + F_{\text{bias}}) + G(q), \tag{22}$$

where F_{bias} is a 6×1 bias force/torque matrix, which can be used for simulation of special effects like virtual weight lifting.

5.4. *Upper limb assistive impedance control*

Under the assistive control mode, the exoskeletal system applies assistive force signals dependent on the operator's desired motion. To enable detection of the user's desired motion, an F/T sensor is mounted at the distal section (endtip) of the exoskeleton. This sensor monitors the force signals applied by the user; Fig. 9. Based on these force signals, the desired position of the system x_E is updated in Eq. (21).

We use the following formula to derive the new desired position using the sensed force signal

$$x_E^i = x_{E-1}^i + \int x_f^i dt, i = 1, \ldots, 6, \tag{23}$$

$$x_f^i = \left\{ \begin{array}{cc} k_a(F_s^i - a) & F_s^i > a \\ 0 & -a < F_s^i < a \\ k_a(F_s^i + a) & F_s^i < -a \end{array} \right\}, \tag{24}$$

where $x_E^i = \left[x_E^1 \cdots x_E^6 \right]^T$ is the desired position vector, $F_s^i = \left[F_s^1 \cdots F_s^6 \right]^T$ is the force vector from the F/T sensor, k_a is a sensitivity coefficient that can be

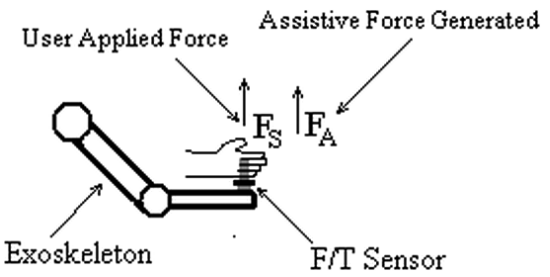

Fig. 9. Assistive mode setup for the exoskeleton arm.

adjusted according to the user's physical state, and a is the deadband parameter. By inserting the desired position vector derived from (23), (24) into (22) the impedance controller described in (22) can generate assistive forces towards the direction of the user motion.

6. Experimental Results

A number of preliminary experiments were carried out to evaluate the performance of the system as a physiotherapy and augmentation device initially for the upper limb. The results are presented in the following sections.

6.1. *Shoulder strengthening with weight training*

The shoulder is considered to be one of the most complex joints of the human body, but it is also one of the most vulnerable to injury. This complexity of movement makes the shoulder joint distinctive from a training and rehabilitation perspective. One group of rehabilitation exercises often used for shoulder training or treatment after injury is based on consistent repetitive motions using small weights. In this experiment, the training exoskeleton was configured to simulate the forces generated by a virtual constant load located at the elbow joint. The arm exoskeleton was securely attached to the operator's arm and the control matrices were set up as follows to simulate a 2 kg load; Fig. 10.

Since the load is located at the elbow frame, the Jacobian up to the elbow was used to resolve the load into shoulder joint torques. During the experiment, the operators repeated a shoulder abduction/adduction exercise as shown in Fig. 10. During these motions, the position and the output torque of the shoulder abduction/adduction joint torque were recorded.

The results introduced in Fig. 11(a) show the abduction/adduction motions for a typical test subject. Graph 11(b) introduces the desired and the output torque of the shoulder abduction/adduction joint as recorded during the experiment.

Graphs 11(c) and 11(d) illustrate the output load as a function of the time and the joint position. The maximum external load error is less than 2.5% for the whole motion range. In terms of the actual sensation, the test subjects (ten male subjects

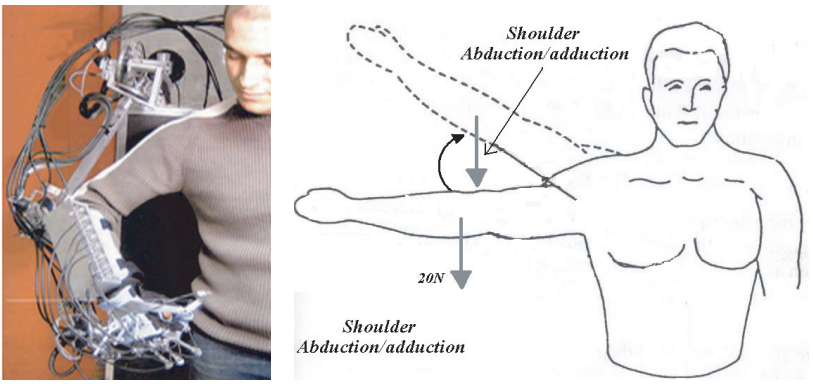

Fig. 10. Shoulder training experiment.

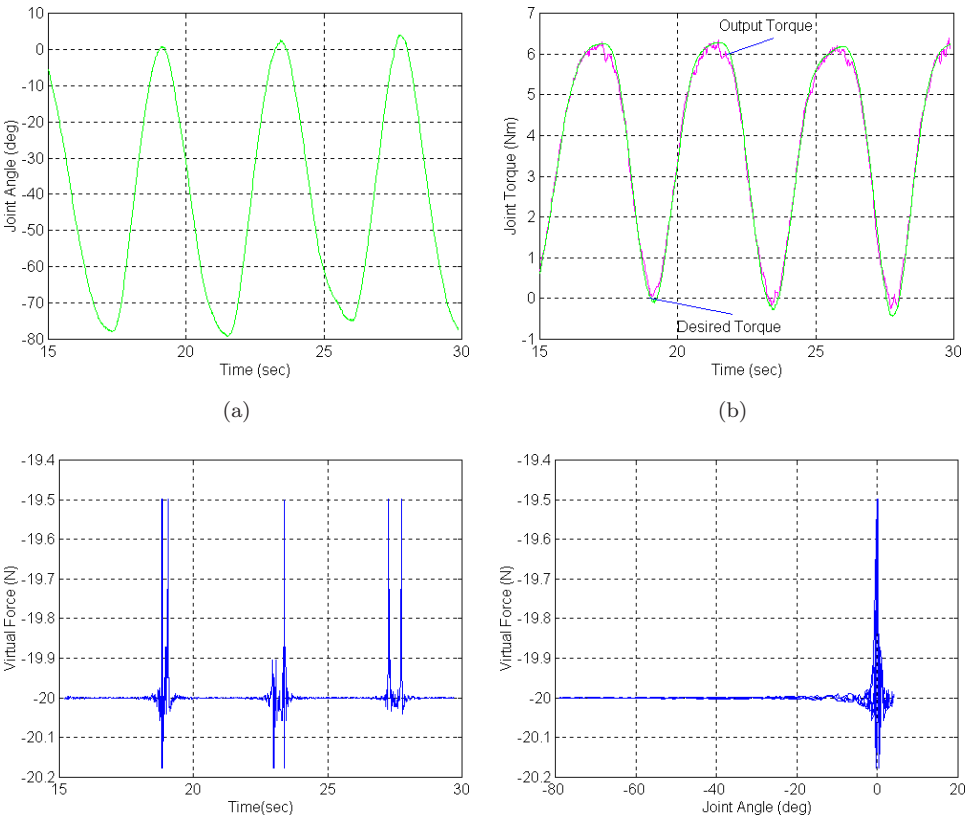

Fig. 11. Shoulder training experimental results.

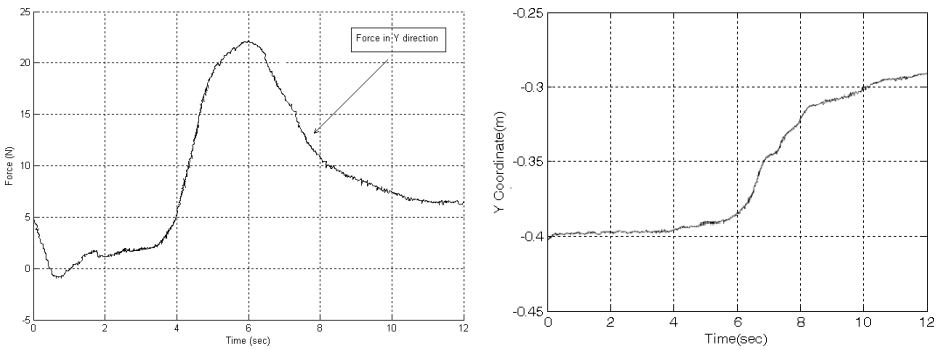

(a) (b)

Fig. 12. (a) Force felt by the user, and (b) assistive motion response.

aged 22–35) reported that the sensation of the external load is very close to the natural sensation, giving very encouraging feedback about the possibility of using the system as a training/rehabilitation device and applying this to a more extensive range of physiotherapy training regimes in addition to applications as a power assist system.

6.2. *Assistive/augmentation mode experiment*

In this experiment, the assistive capacity was assessed by evaluating the performance of the upper limb exoskeleton in providing assistive force signals in healthy subjects. The device was securely attached to the operator's arm and it was configured to work in assistive mode. A load of 2 kg was attached at the exoskeleton endtip and the users were prompted to manipulate the exoskeletal device and try to lift the attached load vertically. During this time, the force sensed at the F/T sensor was recorded. Figure 12(a) shows the force profile sensed by the sensor, which is actually the force felt by the user. The force initially increases as the user starts trying to move the exoskeletal system in order to lift the load. The increase force levels cause changes in the desired vertical y-coordinate [Fig. 12(b)] which subsequently causes assistive forces governed by (22) to be generated at the tip of the system. As a result, the force applied by the user [Fig. 12(a)] decreases. This indicates the capability of the system and the proposed assistive control scheme to provide assistive forces under user's motion control.

7. Conclusions and Further Work

The concepts for exoskeletal systems have been around for some time and the potential for these devices in applications ranging from construction, manufacturing and mining to rescue and emergency services is immense. In recent years, research has been driven by possible uses in medical/rehabilitation and military applications.

Yet despite the obvious benefits from the use of exoskeletons, there still remain barriers to the effective use and exploitation of this technology. One of the most

pertinent of these factors is the power and actuation system. In particular, since an exoskeleton is in essence a robot coupled to a human at several contact points, there are issues of safety and control.

This paper address these issues through the development of lightweight upper and lower body systems that are powered by braided pneumatic muscle actuators (PMAs) which provide systems with high power, good control, accurate motion and compliant behavior that permits a soft, and therefore safer, interaction with the user. The paper has shown the background to the development of the systems, showing a brief history of exoskeletal systems. Based on this, a user requirement has been defined. The paper has shown the design, construction and testing of ultra low mass arm and leg based exoskeletons. These systems are shown to be able to augment the power of users (either able-bodied or unwell) providing up to 100% assistance for seven DOFs in the arm and five DOFs in the legs. Along with the above functionality, the system was designed to meet the specifications of lightness, gravity compensation, ease of fitting and adjustment and relatively low mechanical complexity, which are essential for any system that is in direct contact with the human operator. It has been shown that the system can provide a stable, compact and viable augmentation system for rehabilitation activities involving both arm and leg actions. Results have been introduced to demonstrate the capability of the system as a physiotherapy training facility.

Ongoing research will seek to address several issues related to the individual lower and upper body systems and the combined unit. For the upper limb, future work is addressing rehabilitation post stroke through task based therapies, which is a new technique that shows excellent potential for improved long-term stroke recovery. The use of daily exoskeleton based therapy has shown excellent potential. Studies will also look at the use of the exoskeletons for daily use by those with muscle wastage, permitting increased independence. For the lower limb, the goal is assistive activity post paralysis and stroke. The exoskeleton has been integrated with a tread mill and active body support systems provide graded limb loading during training.

In the non-medical direction, work is ongoing to develop the system to augment power assistance during the execution of simple tasks, such as load lifting or tasks that require repetitive stress motions. This will include the understanding of the power requirements of these tasks and the development of effective force amplification control strategies that will enable the execution of the physical activities.

Further studies will also consider the development of fully independent power sources and increased actuator power for operations involving user power outputs exceeding current physical levels.

References

1. H. Inoue, Whither robotics: Key issues, approaches and applications, in *IEEE Int. Conf. Intelligent and Robots and Systems (IROS)*, Osaka, Japan (IEEE Press, 1996), pp. 9–14.

2. M. Brown, N. Tsagarakis and D. G. Caldwell, Exoskeletons for human force augmentation, *Ind. Robot.* **30**(6) (2003) 592–602.
3. N. Tsagarakis and D. G. Caldwell, Development and control of a "soft-actuated" exoskeleton for use in physiotherapy and training, invited paper for *Autonomous Robots*, Vol. 15 (Kluwer Academic Publishers, 2003, pp. 21–33).
4. M. Vukobratovic, V. Ciric and D. Hristic, Contribution to the study of active exoskeletons, in *Proc. 5th Int. Federation of Automatic Control Congress*, Paris (1972).
5. H. Kazerooni, Human-robot interaction via the transfer of power and information signals, *IEEE Trans. Syst. Cybern.* **20**(2) (1990) 450–463.
6. H. Kazerooni and S. Mahoney, Dynamics and control of robotic systems worn by humans, *ASME J. Dyn. Syst. Measure. Contr.* **13**(3) (1991) 379–387.
7. G. C. Burdea, Force and touch feedback for virtual reality, New York (1996).
8. S. Jacobsen, F. Smith, B. Backman and E. Iversen, High performance, high dexterity for reflective teleoperator II, *Topical Meeting on Robotics and Remote Systems* (ANSI), New York (1991).
9. M. Bergamsco, B. Allotta, L. Bosio, L. Ferreti and G. Parrini, An arm exoskeleton systems for teleoperation and virtual environments applications, *IEEE Int. Conf. Robotics and Automation (ICRA)*, San Diego, USA (IEEE Press, 1994), pp. 1449–1454.
10. S. Lee, S. Park, M. Kim and C. W. Lee, Design of a force reflecting master arm and hand using pneumatic actuators, in *IEEE Int. Conf. Robotics and Automation (ICRA)*, Leuven, Belguim (IEEE Press, 1998), pp. 2574–2579.
11. A. Nakai, T. Ohashi and J. Hashimoto, 7 D.O.F arm type haptic interface for teleoperation and virtual reality systems, in *IEEE Int. Conf. Intelligent and Robots and Systems (IROS)*, Victoria, Canada (IEEE Press, 1998), pp. 1266–1271.
12. H. Kazerooni, Hybrid control of the Berkeley lower extremity exoskeleton (BLEEX), *Int. J. Robot. Res.* **25** (2006) 561–573.
13. E. Guizzo and H. Goldstein, The rise of the body bots, *IEEE Spectrum* (October 2006).
14. M. A. Alexander, M. R. Nelson and A. Shah, Orthotics, adapted seating and assistive devices, in *Pediatric Rehabilitation*, 2nd edn., Baltimore MD (Williams and Wilkins, 1992), pp. 186–187.
15. P. H. Stern and T. Lauko, Modular designed wheelchair based orthotic system for upper extremeties, *Paraplegia* **12** (1975) 299–304.
16. N. Benjuya and S. B. Kenney, Hybrid arm orthosis, *J. Prosthet. Orthot.* **2**(2) (1990) 155–163.
17. K. Homma and T. Arai, Design of an upper limb assist system with parallel mechanism, in *IEEE Int. Conf. Robot. Automat.*, Nagoya, Japan (IEEE Press, 1995), pp. 1302–1307.
18. G. R. Johnson and M. A. Buckley, Development of a new otorised upper limp orthotic system (MULOS), in *Proc. Rehabilitation Engineering Society of North America*, Pittsburgh PA (June 1997), pp. 399–401.
19. A. Yardley, G. Parrini, D. Carus and J. Thorpe, Development of an upper limb orthotic exercise system, *ICRR*, Stanford CA (1997).
20. N. Hogan, H. I. Krebs, J. Charnnarong, P. Srikrishna and A. Sharon, MIT-MANUS: A workstation for manual therapy and training, in *Proc. IEEE Workshop on Robot and Human Communication*, Tokyo, Japan (1992), pp. 161–165.
21. H. I. Krebs, N. Hogan, M. L. Aisen and B. T. Volpe, Robot-aided neuro-rehabilitation, *IEEE Trans. Rehab. Eng.* (1998), pp. 75–87.

22. K. Nagai, I. Nakanishi, H. Hanafusa, S. Kawamura, M. Makikawa and N. Tejima, Development of an 8 D.O.F robotic orthosis for assisting human upper limb motion, *IEEE Int. Conf. Robot. Automat. (ICRA)*, Leuven, Belgium (IEEE Press, 1998), pp. 3486–3491.
23. D. J. Reinkensmeyer, J. P. A. Dewald and W. Z. Rymer, Guidance-based quadification of arm impairment following brain injury, *IEEE Trans. Rehab. Eng.* **7**(1) (March 1999) pp. 1–11.
24. D. J. Reinkensmeyer, L. E. Kahn, M. Averbuch, A. McKenna-Cole., B. D. Schmit and W. Z. Rymer, Understanding and treating arm movement impairment after chronic brain injury: Progress with arm guide, *J. Rehab. Res. Dev.* **37**(6) (November 2000).
25. P. Mark, G. T. Gomes and G. R. Johnson, A robotic approach to neuro-rehabilitation interpretation of biomechanical data, *7th Int. Symp. 3-D Analysis of Human Movement* (July 2002).
26. N. Tsagarakis, D. G. Caldwell and G. A. Medrano-Cerda, A 7 D.O.F pneumatic Muscle Actuators (pMA) powered exosksleton, *Ro-Man*, Pisa, Italy (September 1999), pp. 327–333.
27. H. Z. Tan, M. A. Srinivasan, B. Eberman and B. Cheng, Human factors for the design of force-reflecting haptic interfaces, *Dyn. Syst. Control (ASME)* **55**(1) (1994) 353–359.
28. R. Kalawsky, *The Science of Virtual Reality and Virtual Environments* (Addison Wesley, UK, 1993).
29. I. Sarakoglou, N. Tsagarakis and D. G. Caldwell, Occupational and physical therapy using a hand exoskeleton based exerciser, *IEEE Int. Conf. Intell. Robot. Syst. (IROS)*, Sendai, Japan (IEEE Press, 2004), pp. 2973–2978.
30. S. Kousidou, N. Tsagarakis and D. G. Caldwell, Assistive exoskeleton for task based physiotherapy in 3-dimensional space, *IEEE BioRob 2006*, Pisa, Italy (Feburary 2006).
31. P. Harold, Van Cotte and R. G. Kinkade, *Human Engineering Guide to Equipment Design* (McGraw Hill, 1972).
32. N. Costa, M. Brown, S. Hutchins, J. O. Gray and D. G. Caldwell, Joint motion control of a powered lower limb orthosis for rehabilitation, *Int. J. Automat. Comput.* **3**(3) (2006) 271–281.
33. D. G. Caldwell, G. A. Medrano-Cerda and M. J. Goodwin, Control of pneumatic muscle actuators, *IEEE Control Syst. J.* **15**(1) (1995) 40–48.
34. N. Tsagarakis and D. G. Caldwell, Improved modelling and assessment of pneumatic muscle actuators, *IEEE Int. Conf. Robot. Automat. (ICRA)*, San Fancisco, USA (IEEE Press, 2000), pp. 3641–3646.
35. C. P. Chou and B. Hannaford, Measurement and modeling of McKibben pneumatic artificial muscles, *IEEE Trans. Robot. Automat.* **12**(1) (1996) pp. 90–102.

Darwin G. Caldwell received his B.Sc. and Ph.D. in Robotics from the University of Hull in 1986 and 1990, respectively. In 1994, he received an M.Sc. in Management from the University of Salford. He was at the University of Salford from 1989 to 2007 as a Lecturer, Senior Lecturer, Reader and finally Professor of Advanced Robotics in the Centre for Robotics and Automation (1999–2007). Since 2006, he has been an Honorary Professor in the Schools of Electronics and Computer Science at the University of Wales, Bangor. His research interests include innovative actuators and sensors, haptic feedback, force augmentation exoskeletons, dexterous manipulators,

humanoid robotics, bipedal and quadrapedal robots, biomimetic systems, rehabilitation robotics, telepresence and teleoperation procedures, and robotics and automation systems for the food industry. Dr Caldwell is the author or co-author of over 170 academic papers, four patents and has received awards at several international conference and events. He is a past co-chair of the IEE Robotic and Intelligent Systems and is currently chair of the UKRI region of the IEEE (Robotics and Automation Society) and on the editorial board of *Industrial Robot* (2002–), *International Journal of Systems Science* (1997–2005) and guest editor of several journals.

N. G. Tsagarakis received his Diploma in Electrical Engineering in 1995 from Aristotle University of Thessaloniki in Greece and his M.Sc. and Ph.D. in Advanced Robotics and Haptic Systems Technology in 1997 and 2000, respectively, from the University of Salford in UK. Over the last seven years, he has been a Research Fellow at the Centre of Robotics and Automation at the University of Salford, UK. He is currently a Research Scientist at the Italian Institute of Technology in Genoa within the Robotics Department working in the area of wearable robotics, haptic systems and humanoids robots. His other research interests include medical/rehabilitation robotics, novel actuators, dextrous hands and force/tactile sensing. Dr Tsagarakis is the author or co-author of over 50 academic papers in international journals and conference proceedings.

Sophia Kousidou received her B.Sc. in Informatics from the University of Piraeus, Piraeus, Greece and an M.Sc. in Robotics and Automation from the University of Salford, UK. She is currently a Ph.D. candidate in Robotics and Haptics at the Centre for Robotics and Automation, Department of Computer Science and Engineering, University of Salford, UK. Her research interests include rehabilitation robotics, artificial intelligence, virtual reality, haptics, and intelligent agent architectures. She has also worked on behavior-based control with applications in the coordination of mobile robots as well as on intelligent agent architectures.

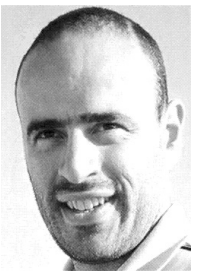

Nelson Costa received his B.Sc degree in Computer and Electronic Engineering in 1995 and his M.Sc. in Robotic Systems and Automation in 1999, both at the University of Coimbra, Portugal. He is currently pursuing his Ph.D. in Advanced Robotics at the University of Salford, UK. His research interests include sensors, actuators, power sources, force augmentation exoskeletons, and rehabilitation robotics.

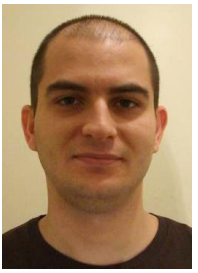

Ioannis Sarakoglou is pursuing a Ph.D. degree in Advanced Robotics at the University of Salford, UK. He holds a B.Eng. degree in Robotics and Electronic Engineering from the University of Salford received in 2002. His research interests include the design and development of portable tactile displays and hand exoskeletons for VR, haptics and rehabilitation applications.